



OPEN

Activity of alkaloids from *Aspidosperma nitidum* against *Leishmania (Leishmania) amazonensis*

Andreza do Socorro Silva da Veiga¹, Fernando Tobias Silveira², Edilene Oliveira da Silva^{3,4}, José Antônio Picanço Diniz Júnior², Sanderson Corrêa Araújo², Marliane Batista Campos², Andrey Moacir do Rosário Marinho⁴, Geraldo Célio Brandão⁵, Valdicley Vieira Vale¹, Sandro Percário^{4,6} & Maria Fâni Dolabela^{1,4}✉

This study evaluated the morphological changes caused by fractions and subfractions, obtained from barks of *Aspidosperma nitidum*, against *L. (L.) amazonensis* promastigotes. The ethanolic extract (EE) obtained through the maceration of trunk barks was subjected to an acid–base partition, resulting in the neutral (FN) and the alkaloid (FA) fractions, and fractionation under reflux, yielded hexane (FrHEX), dichloromethane (FrDCL), ethyl acetate (FrACoET), and methanol (FrMEOH) fractions. The FA was fractionated and three subfractions (SF5-6, SF8, and SF9) were obtained and analyzed by HPLC–DAD and ¹H NMR. The antipromastigote activity of all samples was evaluated by MTT, after that, scanning electron microscopy (SEM) and transmission electron microscopy (TEM) for the active fractions were performed. Chromatographic analyzes suggest the presence of alkaloids in EE, FN, FA, and FrDCL. The fractionation of FA led to the isolation of the indole alkaloid dihydrocorynantheol (SF8 fractions). The SF5-6, dihydrocorynantheol and SF-9 samples were active against promastigotes, while FrDCL was moderately active. The SEM analysis revealed cell rounding and changes in the flagellum of the parasites. In the TEM analysis, the treated promastigotes showed changes in flagellar pocket and kinetoplast, and presence of lipid inclusions. These results suggest that alkaloids isolated from *A. nitidum* are promising as leishmanicidal.

Leishmaniasis is caused by protozoa from the genus *Leishmania*, being endemic in 98 different countries with approximately 350 million people at risk of disease transmission¹, with 94% of new cases arising only in seven of these countries (Brazil, Ethiopia, India, Kenya, Somalia, South Sudan and Sudan)¹.

The treatment is carried out with pentavalent antimonials (Sb5+; N-methyl glucamine-Glucantime® antimoniate and sodium stibogluconate-Pentostan®) and amphotericin B, these are high-cost chemotherapies, used parenterally and usually require a long administration period². Several adverse reactions and toxic effects have been associated with these drugs^{3,4} and some are dose- and time-dependent⁵. In addition, therapeutic failure has been reported, as well as cases of disease recurrence⁶ and parasitic resistance⁷, associated with an intracellular decrease in drug concentration, due to overexpression of ABC carriers^{8,9}.

In this context, it is urgent to search for therapeutic alternatives, and compounds isolated from medicinal plants can be promising¹⁰. Among several possibilities, there are the alkaloids whose leishmanicidal activity has been described in some studies^{11,12}. However, several plant species that present alkaloids have not been studied yet, such as *Aspidosperma nitidum* (Apocynaceae family). Therefore, the present study evaluated whether the fractionation of the ethanolic extract (EE) obtained from trunk barks of *A. nitidum* influenced leishmanicidal activity. The study also evaluated the morphological changes in the parasite caused by the active isolated alkaloids.

¹Postgraduate Program in Pharmaceutical Innovation, Institute of Health Sciences, Federal University of Pará, Belém, PA, Brazil. ²Institute Evandro Chagas, Ananindeua, PA, Brazil. ³Postgraduate Program in Biology of Infectious and Parasitic Agents, Institute of Biological Sciences, Federal University of Pará, Belém, PA, Brazil. ⁴Postgraduate Program in Biodiversity and Biotechnology of the BIONORTE Network, Institute of Biological Sciences, Federal University of Pará, Belém, PA, Brazil. ⁵School of Pharmacy, Federal University of Ouro Preto, Ouro Preto, MG, Brazil. ⁶Oxidative Stress Research Laboratory, Institute of Biological Sciences, Federal University of Pará, Belém, PA, Brazil. ✉email: fani@ufpa.br

Sample	Yields (%)
EE ^a	5.1
FA ^b	29.25
FN ^c	21.8
FrHEX ^d	2.4
FrDCL ^e	8.37
FrACOET ^f	18.6
FrMeOH ^g	38.4

Table 1. Yields of ethanolic extract and its fractions obtained by acid–base partition or reflux extraction. ^aEE:ethanolic extract; ^bFA: alkaloids fraction; ^cFN: neutral fraction; ^dFrHEX: hexane fraction; ^eFrDCL: dichloromethane fraction; ^fFrACOET- ethyl acetate fraction; ^gFrMEOH- methanolic fraction.

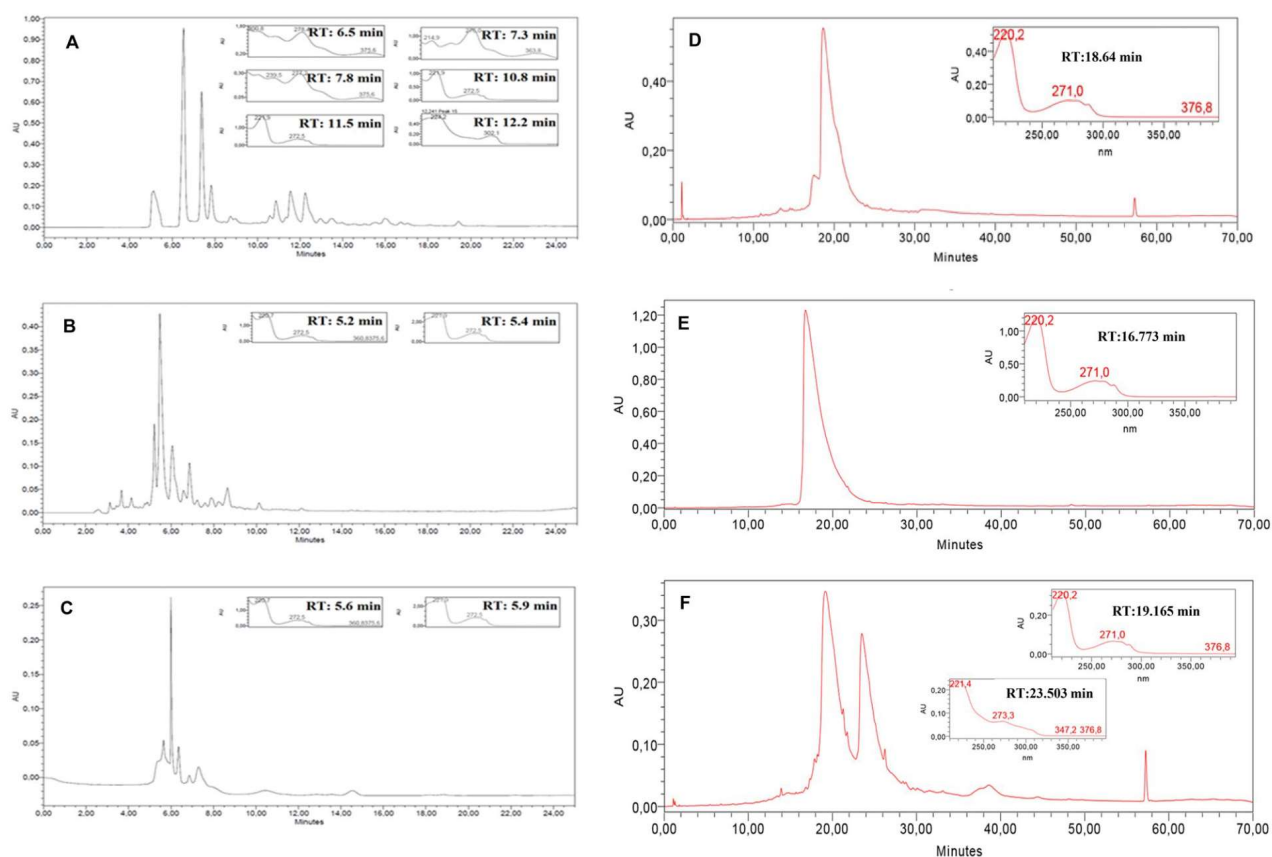


Figure 1. Chromatographic profile and UV spectra of EE, FN, FA and SF5-6, SF8 and SF9 subfractions obtained from *A. nitidum*. Condition: Column RP-18 (45 × 250 mm, 5 μm), λ 220–400 nm, flow = 1 mL/min, temperature > 26 °C. Mobile phase: t = 15 min: 70–30% of eluent B, t = 20 min: 60–40% of eluent B, t = 25 min: 50–100% of eluent B. (A)- EE; (B)- FA; (C)- FN; (D)- SF5-6; (E)- SF8, (F)- SF9.

Results

Phytochemical studies. The yields of EE and fractions are described in Table 1. The analysis in HPLC–DAD detected the presence of alkaloids in the EE (Retention Time (RT)=6.5 min., Maximum Wave-Length (λ_{max}) 200.8; 278.4 and 375.6 nm; RT=7.3 min., λ_{max} 214.9, 276.0 and 363.8 nm; RT=7.8 min., λ_{max} 239.5, 277.2 and 375.6 nm; RT=10.8 min., λ_{max} 221.8 and 272.5 nm; RT=11.5 min., λ_{max} 221.9 and 272.5 nm; RT=12.2 min., λ_{max} 224.2 and 302.1 nm; Fig. 1A), the alkaloid fraction (FA; RT=5.2 and 5.4 min.; λ_{max} 220.7 and 272.5 nm; Fig. 1B), and in the neutral fraction (FN; RT=5.6 and 5.9 min.; λ_{max} 220.7 and 272.5 nm; Fig. 1C), and suggested that subfractions SF 5–6 (RT=18.64 min.; λ_{max} 220.2 and 271.0 nm; Fig. 1D), SF8 (RT=16.773 min.; λ_{max} 220.2 and 271.0 nm; Fig. 1E), and SF9 (RT=19.165 min.; λ_{max} 220.2 and 271.0 nm and RT 23.503 min.; λ_{max} 221.4 and 273.3 nm; Fig. 1F) must be alkaloids.

The analysis of the ¹H NMR spectrum of the SF5-6 subfraction, showed signs of hydrogen with displacements in δH 7.47, 7.35, 7.07, and 7.19 that correspond to aromatic hydrogens. Meanwhile, SF8 ¹H NMR spectrum (see signs below) demonstrated the presence of three signals with chemical shifts in δH 7.40 for H9, δH 7.28 for H12,

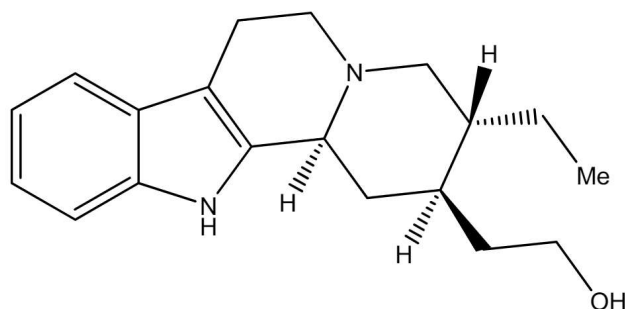


Figure 2. Structure and numbering system of SF8 subfraction (dihydrocorynantheol) based on its biogenesis.

Sample	<i>L. (L.) amazonensis</i>	
	IC ₅₀ ^a (µg/mL) ± SD ^{b(1)}	Activity
SF 5–6	100.3 ± 1.8	Active*
Dihydrocorynantheol	38.4 ± 3.1	Active
SF9	62.4 ± 1.9	Active
FrDCL ^c	105.7 ± 1.1	Moderate
Amphotericin B	0.06 ± 0.002	Active

Table 2. Antipromastigote activities of *Aspidosperma nitidum*. ^aIC₅₀: 50% inhibitory concentration; ^bSD: Standard deviation; ^cFrDCL: dichloromethane fraction; (1) 95% confidence interval.

δH 7.05 for H11 (Fig. 2). The ¹H NMR of the SI9 subfraction showed four δH 7.49, 7.37, 7.15, and 7.06 signals that were attributed to aromatic ring hydrogens.

¹H NMR SF8 (400 MHz, CD₃OD); δ 7.40 (d, Ar-H, H-9), 7.28 (d, Ar-H, H-12), 7.05 (Ar-H, H-11), 6.99 (Ar-H, H-10), 3.68 (m, H-17), 3.49, 3.24 (5H), 3.20 (H-21), 3.03 (6H), 2.80 (6H), 2.77 (d, 5H), 2.52 (d, H-14), 2.30, 2.15 (s), 2.01 (H-16), 1.98 (m), 1.75 (m, H-19'), 1.53 (m), 1.50, 1.35 (m, H-16'), 1.30, 0.94–1.25 (t, H-19).

Anti-promastigote activity and morphological analysis. When considering the antipromastigote activity, Table 2 shows the 50% inhibitory concentrations (IC₅₀%) and that only samples SF5-6, SF-9 and dihydrocorynantheol were active, while FrDCL was moderately active.

In the scanning electron microscopy (SEM) analysis, promastigotes treated with the dichloromethane fraction of EE (FrDCL) displayed alterations in a concentration-dependent fashion. We observed cell rounding, membrane septation and shortening of the flagellum size in parasites treated with 50 µg/mL of FrDCL (Fig. 3F). At a concentration of 25 µg/mL, promastigotes still presented rounded-shape cells (Fig. 3G), and in parasites treated with 12.5 µg/mL, there were no significant changes (Fig. 3H).

Similarly, in parasites treated with SF5-6, SF8, and SF9, as analyzed by SEM, changes were concentration-dependent. For the parasites treated with 50 µg/mL of SF5-6, a short flagellum was observed in most of them, as well as a double flagellum and small protuberances along the flagellum in some of the promastigotes (Fig. 3I), and cell rounding. At the lowest concentration (25 µg/mL), the features displayed were flagellum shortening and cell rounding (Fig. 3J).

The parasites treated with 25 µg/mL of dihydrocorynantheol presented a change in shape of the cell body, which was septate, and flagellum shortening (Fig. 3K). Promastigotes treated with 12.5 µg/mL displayed rounded shape, some displaying cell body septation, but no promastigotes with a short flagellum were observed (Fig. 3L). For the parasites treated with 6.25 µg/mL of dihydrocorynantheol, only rounding cells were observed (Fig. 3M).

Moreover, for the parasites treated with 50 µg/mL of SF9, a round shape and protuberances were observed along the flagellum (Fig. 3N), while at 25 µg/mL there were cells with rounded shape (Fig. 3O), and at 12.5 µg/mL most parasites presented an elongated cell body, a long flagellum, and no protuberances (Fig. 3P).

No significant changes were observed for the negative control group (NC; Fig. 3A), or for the solvent control group (CSOL; Fig. 3B). The main changes caused by the treatment with Amphotericin B were changes in flagellum size, loss of elongated shape, septation of the cell body (0.1953 µg/mL; Fig. 3C). For the promastigotes treated with 0.09765 µg/mL, the same changes were observed, except for the changes in flagellum size (Fig. 3D). The promastigotes treated with 0.048825 µg/mL presented more elongated cells, but septation or flagellum shortening was not observed (Fig. 3E).

Additionally, other groups of promastigotes were treated with the same samples (FrDCL, SF5-6, SF8, and SF9) and the morphological changes were evaluated by transmission electron microscopy (TEM). For the NC, no subcellular changes were observed (Fig. 4A), as well as in the CSOL (Fig. 4B). Parasites treated with FrDCL (50 µg/mL) presented important cellular alterations, such as complete loss of normal morphology, retraction of the cell body, cytoplasmic disorganization, dilated flagellar pocket with evagination of its membrane for possible

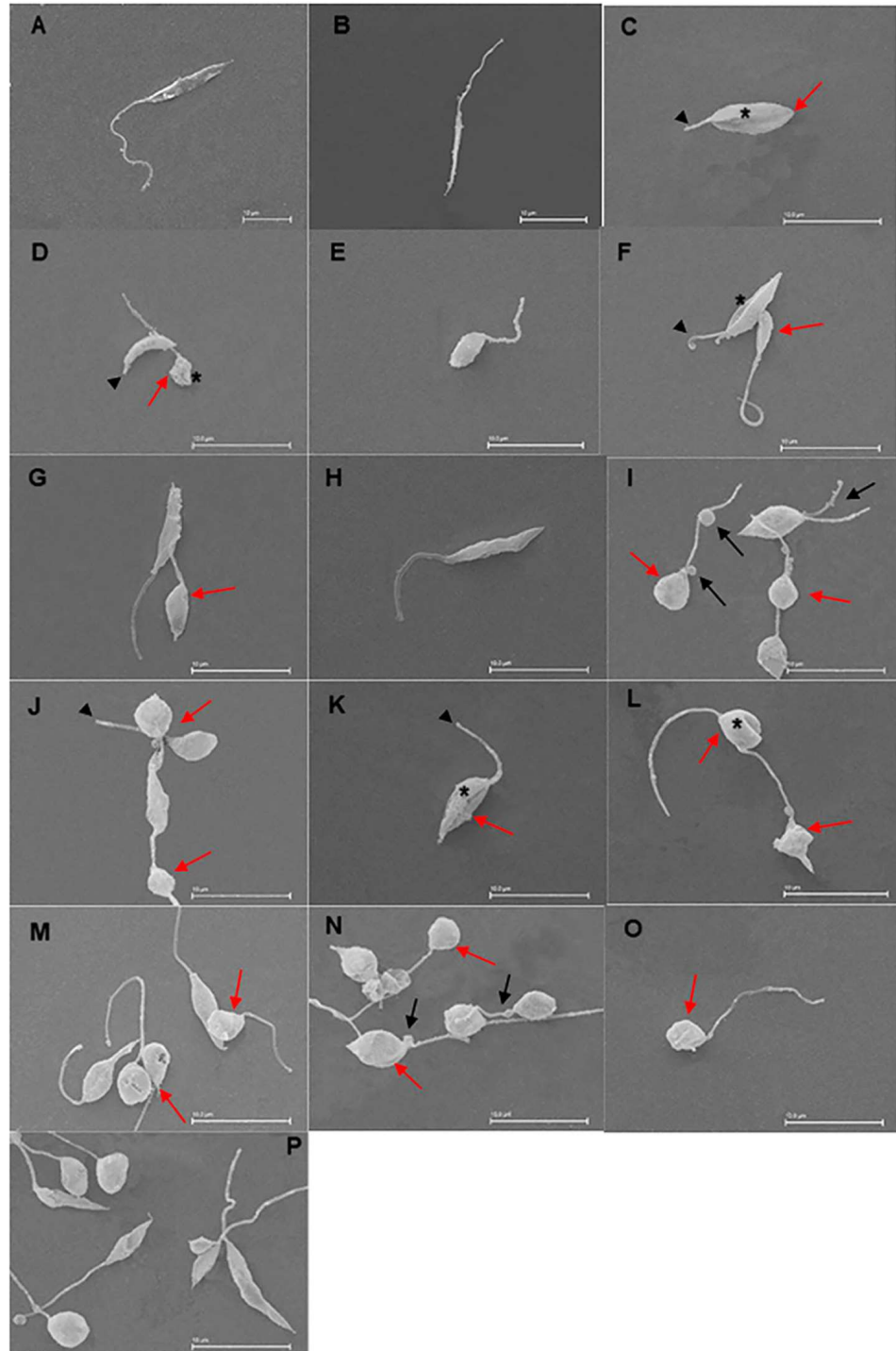


Figure 3. Ultrastructural changes in *L. (L) amazonensis* promastigotes treated with amphotericin B, FrDCL, SF5-6, SF8 and SF9 obtained from *Aspidosperma nitidum* bark. (A) Negative control; (B) Solvent control; (C, D and E) amphotericin B: 0.1953 µg/mL, 0.09765 µg/mL and 0.048825 µg/mL, respectively; (F, G and H) FrDCL: 50 µg/mL, 25 µg/mL and 12.5 µg/mL, respectively; (I and J) SF5-6: 50 µg/mL and 25 µg/mL, respectively; (K, L and M) dihydrocorynantheol: 25 µg/mL, 12.5 µg/mL and 6.25 µg/mL, respectively; (N, O and P) SF9 50 µg/mL, 25 µg/mL and 12.5 µg/mL, respectively. The arrowhead indicates a parasite with a short flagellum, a black arrow indicates protuberances in the flagellum and/or a double flagellum, the red arrow indicates a change in cell shape and the asterisk, septation of the cell body. Bars: 10 µm.

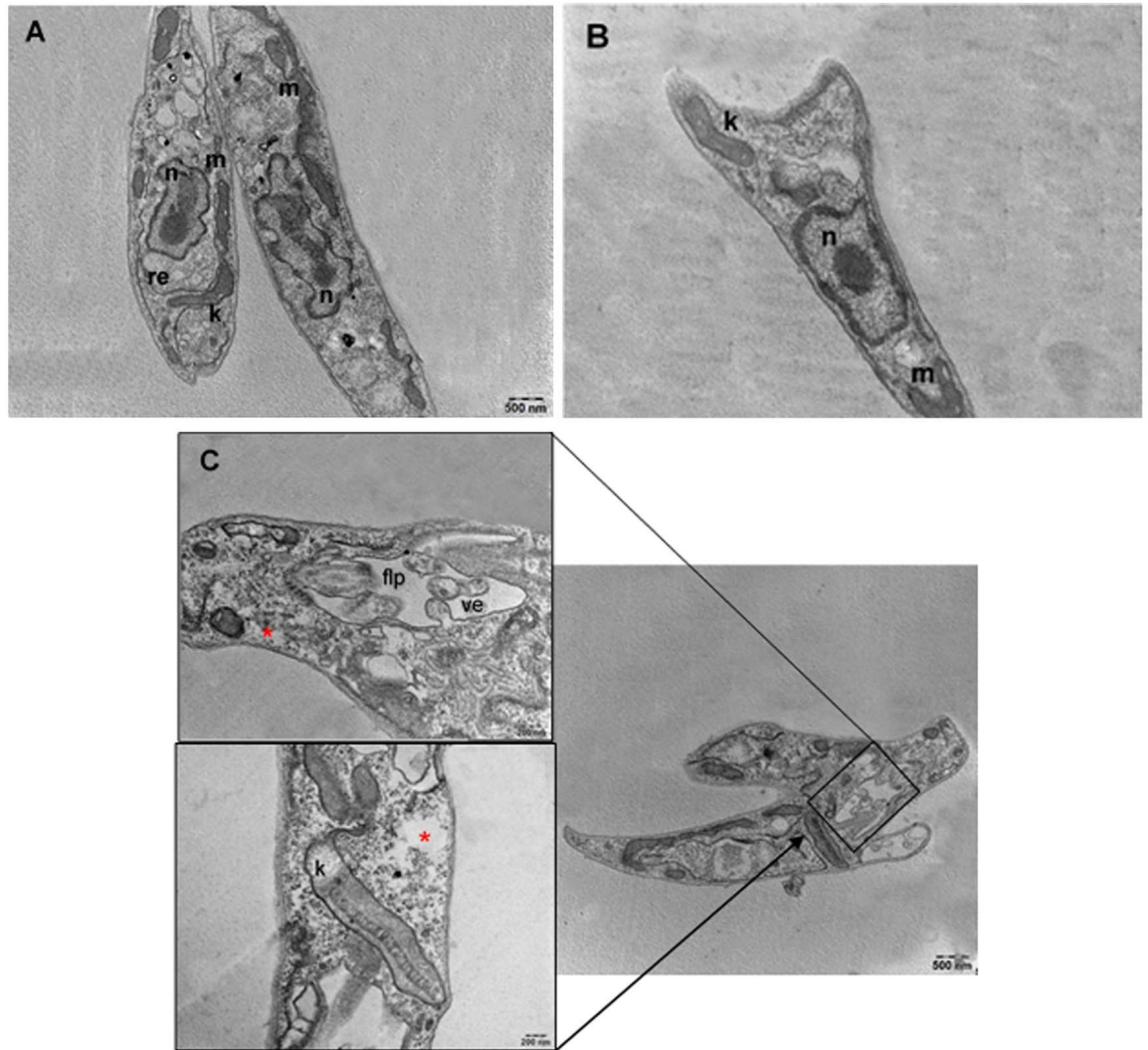


Figure 4. Ultrastructural aspects of *L. (L.) amazonensis* promastigotes untreated and treated with samples for 72 h. (A) Negative control; (B) Solvent control; (C) Promastigotes treated with 50 µg/mL of FrDCL with retraction of the cell body, dilated flagellar pocket with vesicles inside it and presence of vacuoles in the cytoplasm (red asterisk); (D) Promastigotes, treated with 25 µg/mL of FrDCL with rounded cell, lipid inclusion (black arrow), nucleus apparently with fragmented chromatin (red arrow), and vacuoles in the cytoplasm; (E) Promastigotes treated with 12.5 µg/mL of FrDCL with an enlarged flagellar pocket, and alteration in the flagellar membrane (black arrow); (F) Promastigotes treated with 50 µg/mL of SF5-6 presenting dilated flagellar pocket, with vesicles inside, and altered flagellar membrane (red arrow); (G) Promastigotes treated with 25 µg/mL of dihydrocorynantheol, showed retraction of the cell body, dilated flagellar pocket, with vesicles inside and presence of lipid inclusion (black arrow) and vacuoles in the cytoplasm (asterisk); (H) Promastigotes treated with 12.5 µg/mL of dihydrocorynantheol, with changes in the flagellar pocket, with vesicles inside, lipid inclusion (black arrow), dilation of the Golgi complex cisterns. (I) Promastigotes treated with 6.26 µg/mL of dihydrocorynantheol, with a change in the flagellar pocket, with vesicles inside; (J) Promastigotes treated with 50 µg/mL of SF9 with retraction of the cell body, alteration in the flagellar pocket, that has vesicles inside it, vacuoles in the cytoplasm (asterisk), and dilated kinetoplast; (K) Promastigotes treated with 25 µg/mL of SF9 with alteration in the shape of the flagellar pocket, dilated kinetoplast, presence of lipid inclusions and projections of the cytoplasmic membrane (red arrows). (flp) flagellar pocket; (c) chromatin; (gc) Golgi complex; (k) kinetoplast; (fl) flagellum; (lin) lipid inclusions; (m) mitochondria; (n) nucleus; (er) endoplasmic reticulum; (v) vacuoles; (ve) vesicles.

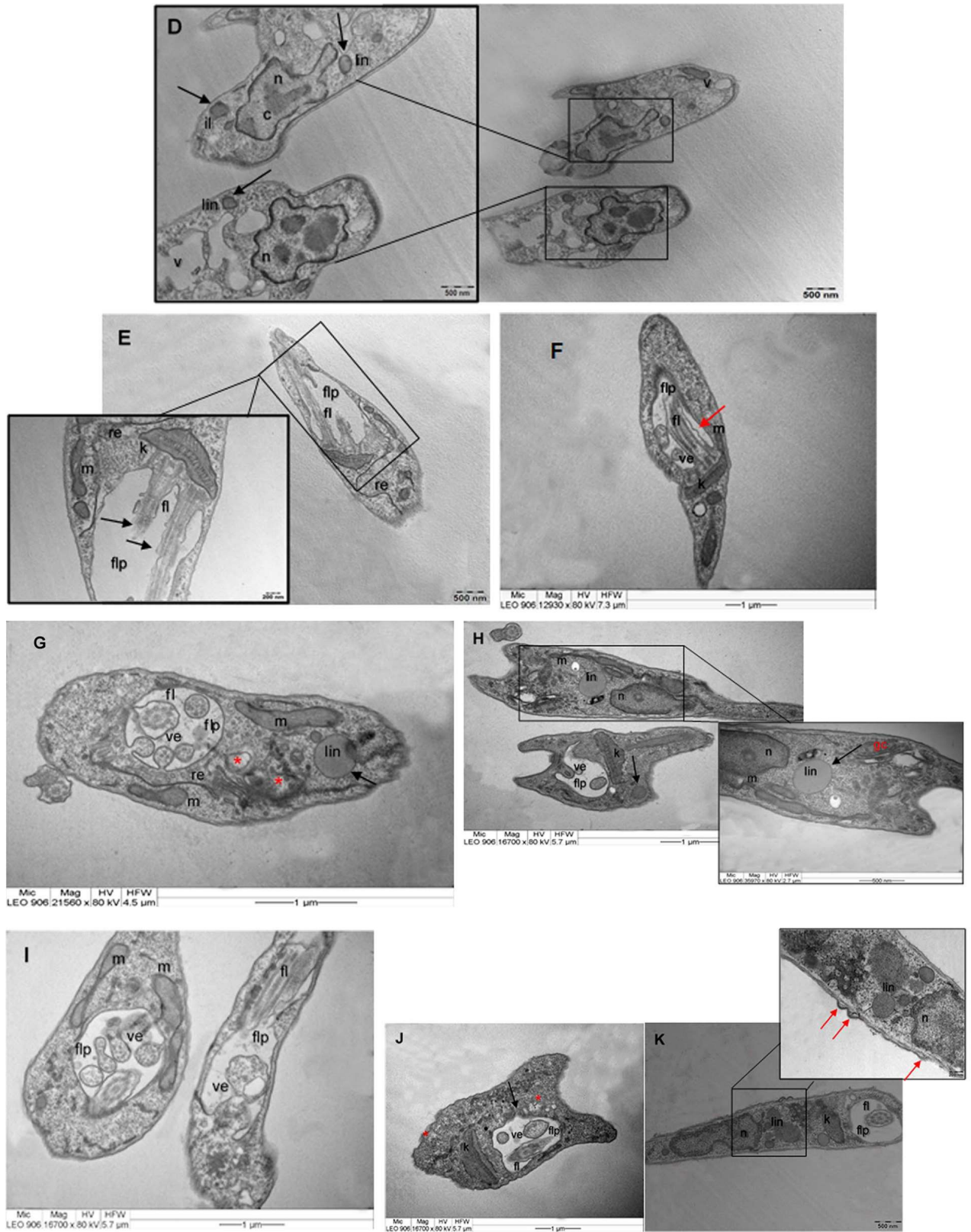


Figure 4. (continued)

formation of vesicles, and cytoplasmic vacuolization (Fig. 4C). The following changes were observed for the parasites treated with 25 µg/mL of FrDCL: rounding cells, lipid accumulation, apparently fragmented chromatin in the nucleus, and an increase in the number of vacuoles in the cytoplasm (Fig. 4D). The treatment of promastigotes with 12.5 µg/mL induced dilatation of the flagellar pocket and alteration in the flagellar membrane (Fig. 4E).

In promastigotes treated with 50 µg/mL of SF5-6, an enlarged flagellar pocket with evagination of its membrane for possible formation of vesicles and alteration of the flagellar membrane were observed (Fig. 4F).

Treatment of promastigotes with 25 µg/mL of dihydrocorynantheol induced cytoplasmic disorganization, cell body retraction, complete loss of normal flagellar pocket morphology with vesicles which were probably results of the evagination of the flagellar pocket membrane, and presence of material with a granular aspect inside these vesicles. In addition to these changes, lipid inclusions and vacuoles were observed in the cytoplasm (Fig. 4G). The treatment of promastigotes with 12.5 µg/mL promoted the appearance of lipid inclusions, changes in the flagellar pocket membrane, which presented vesicles with granular material and were probably the result of this evagination, and dilation of cisterns of the Golgi complex (Fig. 4H). For the promastigotes treated with 6.25 µg/mL, there was also a change in the shape of the flagellar pocket and vesicles within presented granular material (Fig. 4I).

For the promastigotes treated with SF9 at 50 µg/mL, we observed retraction of the cell body, alteration in the flagellar pocket morphology, which contained vesicles with granular material inside, kinetoplast dilation, and the presence of small vacuoles in the cytoplasm (Fig. 4J). Promastigotes treated with 25 µg/mL displayed changes in the flagellar pocket shape, dilated kinetoplast, presence of lipid inclusions, and small projections of the parasite's cytoplasmic membrane (Fig. 4K).

Discussion

To date, no studies that tested the antileishmanial activity of dihydrocorynantheol were found, and this study is the first to test the activity of this indole alkaloid against the parasite of the genus *Leishmania*. Notwithstanding, previous studies isolated different compounds from *A. nitidum*: 10-methoxy-dihydrocorynantheol, corynantheol¹³, harman carboxylic acid¹⁴, 3-methyl-harman-carboxylic acid, dihydrocorynantheol, dehydrositsiriquine¹⁵, and braznitidumine¹⁶. However, none of these alkaloids isolated from *A. nitidum*, and which have a structure similar to dihydrocorynantheol, were tested against species of the genus *Leishmania*, and only one close study was identified, in which the author tested the alkaloid braznitidumine, isolated from the methanolic extract of *A. nitidum*, against the protozoan *Plasmodium falciparum*, but it was inactive¹⁷. In the present study, dihydrocorynantheol (SF8) was isolated, identified, and tested against *L. (L.) amazonensis*, and preliminary analyzes suggest that the other fractions (SF5-6 and SF9) are indole alkaloids, but it was not possible to determine their structure.

After analysis in HPLC–DAD, we believed that the samples where alkaloids and would be promising as leishmanicidal agents, and that fractionation would contribute to this activity. However, only the subfractions (SF5-6; dihydrocorynantheol, and SF-9), which were suggestive of alkaloids, displayed activity against *L. (L.) amazonensis*, whereas the FA was inactive. These results suggest alkaloids isolation is important to antipromastigote activity. Indeed, many alkaloids isolated from plants showed leishmanicidal properties¹⁸.

Some studies describe natural compounds as capable of promoting morphological changes in parasites^{19,20}. The alkaloid β-carboline-1-propionic acid, can induce apoptosis²¹ and it can induce great ultrastructural damage in *L. amazonensis* promastigotes, including some evidence of apoptosis, such as vacuolization of the cytoplasm, presence of myelin-like figures, and swollen kDNA networks²². Another alkaloid, voacamine, induced intense cytoplasm disorganization, presence of autophagic vacuoles, changes in the kinetoplast, mitochondrial membrane, and mitochondrial ridges in promastigotes¹⁹.

Ultrastructural analysis (SEM and TEM) of promastigote forms treated with FrDCL, SF5-6, SF8, and SF9, displayed great morphological changes, which occurred in a concentration-dependent fashion. Despite the fact that FrDCL presented a moderate antipromastigote effect, based on studies developed by members of this research group, and due to the presence of metabolites other than alkaloids in this fraction, we decided to include it in this study to check whether the combination of molecules could promote a different set of morphological changes upon the parasites, than the isolated alkaloids.

In this sense, the morphological analysis revealed that parasites treated with FrDCL presented changes in shape, in the flagellar pocket, and in the cytoplasm. The reduction in concentration contributed to damage reduction, causing dilation of the flagellar pocket and alteration in the flagellar membrane. The FrDCL fraction externalization by the parasite through vesicles resulting from the evagination of the flagellar pocket membrane, suggests that this sample, perhaps, could inhibit hydrolytic^{23,24} or proteolytic enzymes²⁵ and thus be responsible for the damage to the parasite. However, further investigations are needed to elucidate the possible mechanism of action.

Studies reported that endocytosed material is internalized from the flagellar pocket, and then vesicles sprout out from the pocket membrane. These vesicles appear to fuse and discharge their content into intracellular organelles comparable to the endosomes of mammalian cells^{23,24}. There is little information about the factors that control access to the flagellar pocket, and about the physical and biochemical properties of constituents of the pocket lumen. The presence of certain hydrolases (eg, acid phosphatase) within the lumen of the flagellar pocket is an indication that the pocket may act as a prelysosomal hydrolytic compartment^{23,24}.

When considering the study about microorganism proteases, it is important to keep in mind that these enzymes play important roles in the physiology of these organisms, as well as in the pathologies caused by them²⁶. Among them, cysteine proteases are the most investigated proteolytic enzymes in *Leishmania*. These enzymes play important roles in *Leishmania*, such as virulence, viability maintenance, parasite morphology, invasion of the host's mononuclear phagocytic system, and the modulation of its immune response^{27,28}, thus constituting attractive targets for chemotherapy for the treatment of leishmaniasis.

Studies carried out the purification and biochemical characterization of three serine proteases from *Leishmania (L.) amazonensis* promastigotes called LSP²⁹, restricted mainly to intracellular compartments³⁰, as megasomes and to the flagellar pocket³¹.

Protease activity can be regulated in cells or organisms in different ways, including protease inhibition through specific inhibitors³². These inhibitors are valuable tools for investigating the biochemical properties and biological functions of proteases³³ and the inhibition of these enzymes by specific inhibitors can be an important strategy in the production of potent antimicrobial agents³⁴.

When analyzed by TEM, the *L. (L.) amazonensis* promastigotes treated with 10–5 M of the protease inhibitor ShPI-I, obtained from the sea anemone *Stichodactyla helianthus*, presented flagellar pocket with vesicles inside, in addition to bubble formations in the membrane of its pocket, a structure of intense exocytic/endocytic activities. In the cytoplasm, the presence of vesicles that resemble autophagic vacuoles was observed, and this would be a result of intense exocytic/endocytic activity induced by this inhibitor. Moreover, all parasites exhibited changes in shape²⁵. These changes were not seen in control cells. Thus, other classic protease inhibitors such as N-tosyl-L-phenylalanine chloromethyl ketone (TPCK) and benzamidine (Bza) were tested in this study and they also caused changes in the flagellar pocket. In another study, it was observed that ultrastructural abnormalities in the flagellar pocket and lysosome/endosome were seen exclusively with cysteine protease inhibitors regardless of their chemical composition, for example vinyl sulfone *versus* dihydrazide. This observation suggests that the cellular alterations seen are due specifically to inhibition of the cysteine proteases of *Leishmania*²⁷.

We highlight that changes in the flagellar pocket and parasites shape were also observed in the present study. However, whether these enzymes participate in the exocytosis/endocytosis pathway through the processing of intracellular proteins or even in the morphological maintenance of *Leishmania* remains to be elucidated²⁵.

Similar to FrDCL, treatment with a lower concentration of SF5-6 promoted changes in the shape of the flagellar pocket, which presented vesicles with granular material. Increasing the concentration of treatments increased the intensity and occurrence of damage.

The promastigotes treated with FrDCL and SF5-6 presented lipid inclusions. The biogenesis of lipid bodies is involved in cellular homeostasis in eukaryotes, as well as during infection by intracellular pathogens³⁵. Given the role in cellular homeostasis, the accumulation of lipid bodies observed in the treated parasites may be a result of cellular disturbances and loss of homeostasis. Moreover, the intracellular presence of lipid bodies can indicate changes in the content of phospholipids and sterols³⁶.

Similarly, changes in flagellar pocket were observed in parasites treated with dihydrocorynantheol. In addition, the retraction of the cell body of the parasites was observed, which is an alteration frequently detected in apoptotic cells³⁷. During the initial stages of apoptosis, rounding and retraction of the cell is observed. This occurs due to constituent's proteolysis of the cytoskeleton³⁸, facts that were observed in the present study.

Among other changes caused by dihydrocorynantheol, there is the dilation of cisterns in the Golgi complex. This organelle is essential for the processing of lipids and proteins from the endoplasmic reticulum (ER)³⁹. Like the endoplasmic reticulum, the Golgi complex can trigger the apoptotic process in response to stressful situations (excess of proteins unfolded from the endoplasmic reticulum, changes in membrane traffic or in its structure, among others). Some studies demonstrate that the Golgi complex not only suffers the consequences of the apoptotic process, but also plays an active role in the triggering of this type of cell death⁴⁰. All of this reinforces the hypothesis that the leishmanicidal mechanism of dihydrocorynantheol should involve apoptosis.

In the treatment of promastigotes with the SF9, changes in shape, flagellar pocket, kinetoplast, presence of vacuoles, lipid inclusions and small projections of the parasite's cytoplasmic membrane were observed. Most changes are similar to the ones induced by other alkaloids and FrDCL. It is worth mentioning that treatment with SF9 induced the alteration in the kinetoplast of the parasites. This change can be a result of the fragility of the surrounding mitochondrial membrane. Thus, changes in the mitochondrial membrane could indirectly explain the changes observed in the kinetoplast⁴¹. The kinetoplast appears physically associated with the mitochondrial membrane and the basal body by thin filaments, which forms a complex structure known as the tripartite binding zone, which is essential for the positioning of the mitochondrial genome and its correct segregation during cell division⁴².

Conclusion

In this study, alkaloids isolated from *A. nitidum* are promising as leishmanicidal and changes in flagellar pocket may be involved in this activity. Among alkaloids, the most promising is dihydrocorynantheol and, perhaps, apoptosis is involved in this activity. However, further studies need to be carried out to confirm the occurrence of this process in these parasites, since specific markers for apoptosis were not used in this investigation.

Methods

Plant material. The bark of *A. nitidum*, locally known as Caranapauba were collected in Santa Bárbara do Pará, PA-Brazil (S 01° 10 '946' W 048° 11 '715') during May 2013. The plant material was identified by Dra. Rafaela Trindade and the exsiccate was incorporated into the MG Herbarium of the Museu Paraense Emílio Goeldi, under no. MG206608. In the present study we used a wild plant collected from a virgin forest of the Amazon, and our work posed no risk of extinction for the species. During the collection, we took all care to remove the barks so as not to cause any damage to the species, in addition, only a small proportion of the barks were collected. The species were kept integrated and survived the collection. The project complies with national and international guidelines and legislation and is registered on the platform of the national management and Genetic Heritage System and Associated Traditional Knowledge (SISGEN), whose provided license to collect the species under registration A92C186.

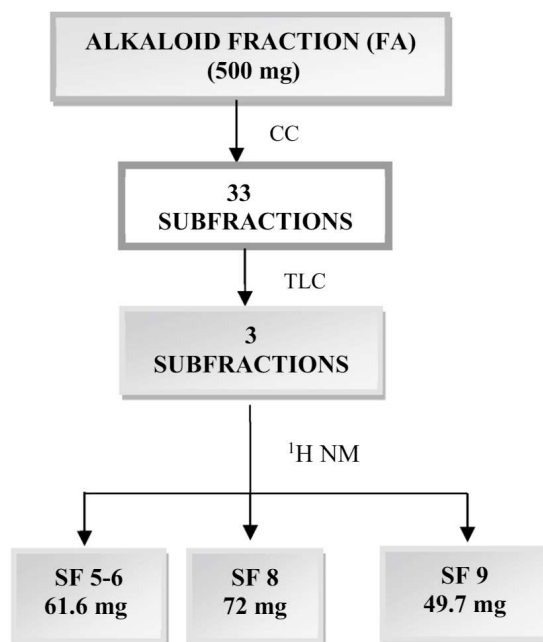


Figure 5. Flowchart for obtaining SF 5–6, SF8 and SF9 subfractions.

Phytochemical studies. The trunk barks of *A. nitidum* were dried in an oven (40 °C for 7 days; Medicate Medical Products, model MD 1.2), grounded, and subjected to maceration (7 days) to obtain the EE, which was subjected to an acid–base partition, resulting in the neutral (FN) and alkaloid fractions (FA)⁴³. The EE was also subjected to extraction under reflux, yielding the following fractions: hexane (FrHEX), dichloromethane (FrDCL), ethyl acetate (FrAcOEt) and methanol (FrMeOH)⁴⁴.

The FA (500 mg) was subjected to fractionation in an open silica gel chromatographic column (CC; 63–200 mm; Macherey–Nagel), using mobile phases of increasing polarity (dichloromethane, ethyl acetate e methanol; Quimis; Isofar) resulting in 33 subfractions which were analyzed in Thin Layer Chromatography (TLC) on silica gel (Macherey–Nagel) and combined, resulting in three subfractions to SF5–6, SF8 and SF9 (Fig. 5). Structural identification was performed by hydrogen nuclear magnetic resonance (¹H NMR; Bruker Ascend 400) at 25°C, using deuterated methanol (MeOD; Sigma–Aldrich[®]) to solubilize the samples. Thus, EE, fractions and subfractions were analyzed by High Performance Liquid Chromatography coupled to a Diodes Array Detector (Waters e2695 and Waters 2998).

The analysis was performed in a RP 18 column (45 × 250 mm, 5 μm), using a mixture of water acidified with 0.01% of trifluoroacetic acid (eluent A; Tédia) and acetonitrile acidified with 0.01% of trifluoroacetic acid (eluent B; Tédia) as the mobile phase. A linear elution gradient was used: 70–30% of eluent B for 15 min, 60–40% of eluent B for 20 min and 50–100% of eluent B for 25 min. The temperature was maintained above 26 °C, flow of 1 mL/min, UV detection at 220–400 nm⁴³.

Antipromastigote activity. The promastigote form of *Leishmania (L.) amazonensis* (MHOM/BR/2009/M26361) was grown in NNN medium (Novy–Nicolle–Mcneal) and later transferred to RPMI (Roswell Park Memorial Institute medium; Gibco) supplemented with 10% of denatured fetal bovine serum (Cultilab materials for cell culture), penicillin G 10,000 IU (Gibco)/mL and streptomycin 10,000 μg (Gibco)/mL and maintained at 25 °C ± 1 °C through weekly passages. In the assay of antipromastigote activity, promastigotes were quantified in a Neubauer chamber (Improved) and then distributed in cell culture plates (Techno Plastic Products–TPP), previously pre-dosed with different concentrations of the samples and amphotericin B (positive control; Cristália pharmaceutical products). The plates were incubated and after 72 h of treatment, the tetrazolium salt (Sigma–Aldrich) was added followed by a new incubation. After 4 h of incubation, dimethyl sulfoxide (Dinâmica) was added and, then, the reading was performed in a microplate reader (Biotek, model ELX 808) at 490 nm. The samples were considered active when the IC₅₀ ≤ 100 μg/mL, moderately active IC₅₀ 101–200 μg/mL, inactive when the IC₅₀ ≥ 200 μg/mL as adapted from⁴⁵. The 50% Inhibitory Concentration (IC₅₀) is the concentration that causes a 50% reduction in growing cells (viable) and was determined by the GraphPad Prism software.

Morphological analysis. The parasites treated with the active samples were analyzed by SEM (LEO 1450 VP) and TEM (ZEISS model EM 906 e ZEISS model EM 900), according to the method described by⁴⁶.

In SEM analysis, promastigotes (4 × 10⁶ parasites/500 μL) were distributed in 24-well plates (TPP) pre-dosed with FrDCL, SF5–6, SF8 and SF9 (50 μL/well), after that they were incubated 72 h/26 °C. Afterwards, the contents of each well were removed, centrifuged and then fixed in PHEM (PIPES—piperazine-n n'-bis(2-ethanesulfonic acid) 20 mM, EGTA (Ethylene glycol-bis(β-aminoethyl ether)-N,N,N',N'-tetraacetic acid tetrasodium salt)

10 mM, MgCl₂ (Magnesium chloride) 5 mM, KCl (Potassium chloride) 70 mM 1X) + Paraformaldehyde (PFA; Electron Microscopy Sciences) 4% + 2.5% glutaraldehyde in 0.1 M sodium cacodylate buffer (Electron Microscopy Sciences), pH 7.2 for 2 h. Then, the parasites were washed with 0.1 M sodium cacodylate buffer (pH 7.2) and deposited in glass coverslips with a solution of 0.1% poly-L-lysine (Sigma-Aldrich, St. Louis) for 2 h.

Post-fixation was performed with a solution containing 1% osmium tetroxide (Sigma-Aldrich, St. Louis) and potassium ferrocyanide (Electron Microscopy Sciences) for 1 h. Then, the coverslips were washed with 0.1 M sodium cacodylate buffer, pH 7.2, dehydrated in a graded ethanolic series (70, 80, 90 and 100%; Merck) and dried by the critical point method using CO₂. The samples on the coverslips were fixed on an appropriate support and metallized with a platinum film for about 2 min. The parasites were analyzed by SEM (LEO 1450 VP).

In the TEM analysis, the parasites were centrifuged, and the pellet resuspended in a 1% glutaraldehyde solution with 4% paraformaldehyde in 0.1 M PHEM buffer (pH 7.4), and 2.5% sucrose for fixation for 1 h. After fixation, the cells were washed with 0.1 M sodium cacodylate buffer (pH 7.4) and post-fixed in a solution containing 1% osmium tetroxide and 1% potassium ferrocyanide for 1 h in the dark, washed with buffer 0.1 M cacodylate (pH 7.4), and then with distilled water and immersed in a contrasting 1% uranyl acetate (Electron Microscopy Sciences) solution in 25% acetone (MERCK) for 1 h. Then, samples were dehydrated in graded acetone (50, 70, 90 and 100%). Afterwards, the cells were slowly impregnated in increasing concentrations of Epon (Electron Microscopy Sciences) diluted in acetone until pure Epon (100%). The samples were then infiltrated with pure Epon + DMP-30 (2,4,6-Tris (dimethylaminomethyl) phenol) and left in a support for polymerization in an oven at 60 °C for 48 h. The blocks were cut in an ultramicrotome (Leica, model EMVC6) and ultrathin sections were contrasted with 5% uranyl acetate and, subsequently, with lead citrate for further analysis by TEM (ZEISS model EM 906 and ZEISS model EM 900).

Received: 11 December 2021; Accepted: 2 March 2022

Published online: 23 May 2022

References

1. PAHO (Pan American Health Organization). Información general: Leishmaniasis. http://www.paho.org/hq/index.php?option=com_content&view=article&id=417:2014-informacion-general-leishmaniasis&Itemid (2018).
2. Sundar, S. & Chakravarty, J. Liposomal amphotericin B and Leishmaniasis: dose and response. *J. Glob. Infect. Dis.* **2**, 159–166. <https://doi.org/10.4103/0974-777X.62886> (2010).
3. Chulay, J. D., Spencer, H. C. & Mugambi, M. Electrocardiographic changes during treatment of leishmaniasis with pentavalent antimony (sodium stibogluconate). *Am. J. Trop. Med. Hyg.* **34**, 702–709. <https://doi.org/10.4269/ajtmh.1985.34.702> (1985).
4. Croft, S. L. & Yardley, V. Chemotherapy of leishmaniasis. *Curr. Pharm. Des.* **8**(4), 319–342. <https://doi.org/10.2174/1381612023396258> (2002).
5. Franke, E. D. *et al.* Efficacy and toxicity of sodium stibogluconate for mucosal leishmaniasis. *Ann. Int. Med.* **113**, 934–940. <https://doi.org/10.7326/0003-4819-113-12-934> (1990).
6. Padrón-Nieves, M. & Ponte-Sucre, A. Marcadores de resistencia en *Leishmania*: susceptibilidad in vitro a drogas leishmanicidas vs retención de calceína en aislados de pacientes venezolanos con leishmaniasis cutánea difusa. *Arch. Venez. Farmacol. y Ter.* **34**, 53–57 (2015).
7. Sundar, A. S. & Goyal, N. Molecular mechanisms of antimony resistance in *Leishmania*. *J. Med. Microbiol.* **56**, 143–153. <https://doi.org/10.1099/jmm.0.46841-0> (2007).
8. Blackmore, C. G., McNaughton, P. A. & Veen, H. W. V. Multidrug transporters in prokaryotic and eukaryotic cells: physiological functions and transport mechanisms. *Mol. Membr. Biol.* **18**, 97–103. <https://doi.org/10.1080/09687680010030200> (2001).
9. Leslie, E. M., Deeley, R. G. & Cole, P. C. Multidrug resistance proteins: role of P-glycoprotein, MRP1, MRP2 and BCRP (ABCG2) in tissue defense. *Toxicol. Appl. Pharmacol.* **204**, 216–237. <https://doi.org/10.1016/j.taap.2004.10.012> (2005).
10. Carvalho, P. B. & Ferreira, E. I. Leishmaniasis phytotherapy. Nature's leadership against an ancient disease. *Fitoterapia* **72**, 599–618. [https://doi.org/10.1016/S0367-326X\(01\)00301-X](https://doi.org/10.1016/S0367-326X(01)00301-X) (2001).
11. Ferreira, I. C. P. *et al.* Anti-leishmanial activity of alkaloidal extract from *Aspidosperma ramiflorum*. *Mem. Inst. Oswaldo Cruz* **99**, 325–327. <https://doi.org/10.1590/S0074-02762004000300015> (2004).
12. Silva-Silva, J. V. *et al.* Flavopereirine—an alkaloid derived from *Geissospermum vellosii*—presents leishmanicidal activity in vitro. *Molecules* **24**, 1–13. <https://doi.org/10.3390/molecules24040785> (2019).
13. Arndt, R. R. *et al.* Alkaloid studies-LVIII: the alkaloids of six *Aspidosperma* species. *Phytochemistry* **6**, 1653–1658. [https://doi.org/10.1016/S0031-9422\(00\)82898-8](https://doi.org/10.1016/S0031-9422(00)82898-8) (1967).
14. Pereira, M. M. *et al.* Constituintes químicos e estudo biológico de *Aspidosperma nitidum* (Apocynaceae). *Rev. Bras. Pl. Med.* **8**, 1–8. https://www1.ibb.unesp.br/Home/Departamentos/Botanica/RBPM-RevistaBrasileiradePlantasMedicinais/artigo1_v8_n3.pdf (2006).
15. Nascimento, P. C., Araújo, R. M. & Silveira, E. R. Aplicação da CLAE na análise fitoquímica de *Aspidosperma nitidum*. In: *Reunião Anual da Sociedade Brasileira de Química*. (Águas de Lindóia). <https://sec.s bq.org.br/cdrom/32ra/resumos/T2285-2.pdf> (2006).
16. Pereira, M. M., Alcântara, A. F. C., Piló-Veloso, D. & Raslan, D. S. NMR structural analysis of Braznitidumine: a new indole alkaloid with 1,2,9-triazabicyclo [7.2.1] system, isolated from *Aspidosperma nitidum* (Apocynaceae). *J. Braz. Chem. Soc.* **17**(7), 1274–80. <https://doi.org/10.1590/S0103-50532006000700012> (2006).
17. Coutinho, J. P. *et al.* *Aspidosperma* (Apocynaceae) plant cytotoxicity and activity towards malaria parasites. Part I: *Aspidosperma nitidum* (Benth) used as a remedy to treat fever and malaria in the Amazon. *Mem. Inst. Oswaldo Cruz* **108**(8), 974–982. <https://doi.org/10.1590/0074-0276130246> (2013).
18. Mishra, B. B., Kale, R. R., Singh, R. K. & Tiwari, V. K. Alkaloids: future prospective to combat leishmaniasis. *Fitoterapia* **80**, 81–90. <https://doi.org/10.1016/j.fitote.2008.10.009> (2009).
19. Chowdhury, S. R. *et al.* Voacamine alters *Leishmania* ultrastructure and kills parasite by poisoning unusual bi-subunit topoisomerase IB. *Biochem. Pharmacol.* **138**, 19–30. <https://doi.org/10.1016/j.bcp.2017.05.002> (2017).
20. Rodrigues, A. P. D. *et al.* A novel function for kojic acid, a secondary metabolite from *Aspergillus* fungi, as antileishmanial agent. *PLoS One* **9**, 259. <https://doi.org/10.1371/journal.pone.0091259> (2014).
21. Lala, S., Pramanick, S., Mukhopadhyay, S., Bandyopadhyay, S. & Basu, M. K. Harmine: evaluation of its antileishmanial properties in various vesicular delivery systems. *J. Drug Target.* **12**, 165–175. <https://doi.org/10.1080/10611860410001712696> (2004).
22. Gabriel, R. S. *et al.* β-Carboline-1-propionic acid alkaloid: antileishmanial and cytotoxic effects. *Rev. Bras. Farmacogn.* **29**, 6755–6762. <https://doi.org/10.1016/j.bjp.2019.08.002> (2019).
23. Bates, P. A., Hermes, I. & Dwyer, D. M. *Leishmania donovani*: immunochemical localization and secretory mechanism of soluble acid phosphatase. *Exp. Parasitol.* **68**, 335–46. [https://doi.org/10.1016/0014-4894\(89\)90115-x](https://doi.org/10.1016/0014-4894(89)90115-x) (1989).

24. Bates, P. A., Hermes, I. & Dwyer, D. M. Golgi-mediated post-translational processing of secretory acid phosphatase by *Leishmania donovani* promastigotes. *Mol. Biochem. Parasitol.* **39**, 247–55. [https://doi.org/10.1016/0166-6851\(90\)90063-R](https://doi.org/10.1016/0166-6851(90)90063-R) (1990).
25. Silva-López, R. E., Morgado-Díaz, J. A., Chávez, M. A. & De Simone, S. G. Effects of serine protease inhibitors on viability and morphology of *Leishmania (Leishmania) amazonensis* promastigotes. *Parasitol. Res.* **101**, 1627. <https://doi.org/10.1007/s00436-007-0706-> (2007).
26. Silva-López, R. E. Proteases de *Leishmania*: novos alvos para o desenvolvimento racional de fármacos. *Quím. Nova* **33**, 1541–1548. <https://doi.org/10.1590/S0100-40422010000700022> (2010).
27. Selzer, P. M. *et al.* Cysteine protease inhibitors as chemotherapy: Lessons from a parasite target. *Proc. Natl. Acad. Sci.* **96**, 11015–11022. <https://doi.org/10.1073/pnas.96.20.11015> (1999).
28. Mottram, J. C., Coombs, G. H. & Alexander, J. Cysteine peptidases as virulence factors of *Leishmania*. *Curr. Opin. Microbiol.* **7**, 375–381. <https://doi.org/10.1016/j.mib.2004.06.01> (2004).
29. Silva-Lopez, R. E. & De Simone, G. S. A serine protease from a detergent-soluble extract of *Leishmania (Leishmania) amazonensis*. *Z. Naturforsch* **59**, 590–598. <https://doi.org/10.1515/znc-2004-7-825> (2004).
30. Morgado-Díaz, J. A. *et al.* Subcellular localization of an intracellular serine protease of 68 kDa in *Leishmania (Leishmania) amazonensis* promastigotes. *Mem. Inst. Oswaldo Cruz* **100**, 377–385. <https://doi.org/10.1590/S0074-02762005000400007> (2005).
31. Silva-López, R. E., Morgado-Díaz, J. A., Alves, C. R., Córte-Real, S. & De Simone, S. G. Subcellular localization of an extracellular serine protease in *Leishmania (Leishmania) amazonensis*. *Parasitol. Res.* **93**, 328. <https://doi.org/10.1007/s00436-004-1144-2> (2004).
32. Otlewski, J., Krowarsch, D. & Apostoluk, W. Protein inhibitors of serine proteinases. *Acta Biochim. Polonica* **46**, 532–565 (1999).
33. McKerrow, J. H., Engel, J. C. & Caffrey, C. R. Cysteine protease inhibitors as chemotherapy for parasitic infections. *Bioorg. Med. Chem.* **7**, 639–644. [https://doi.org/10.1016/s0968-0896\(99\)00008-5](https://doi.org/10.1016/s0968-0896(99)00008-5) (1999).
34. Pupkins, M. F. & Coombs, G. H. Purification and Characterization of Proteolytic Enzymes of *Leishmania mexicana mexicana* amastigotes and promastigotes. *J. Gen. Microbiol.* **130**, 2375–2383. <https://doi.org/10.1099/00221287-130-9-237> (1984).
35. Bozza, P. T., Melo, R. C. & Bandeira-Melo, C. Leukocyte lipid bodies regulation and function: contribution to allergy and host defense. *Pharmacol. Ther.* **113**, 30–49. <https://doi.org/10.1016/j.pharmthera.2006.06.006> (2007).
36. Godinho, J. L. P., Georgikopoulou, K., Calogeropoulou, T., De Souza, W. & Rodrigues, J. C. A novel alkyl phosphocholine-dinitroaniline hybrid molecule exhibits biological activity in vitro against *Leishmania amazonensis*. *Exp. Parasitol.* **135**, 153–165. <https://doi.org/10.1016/j.exppara.2013.06.015> (2013).
37. Jiménez-Ruiz, A. *et al.* Apoptotic markers in protozoan parasites. *Parasites Vectors* **3**, 1–15. <https://doi.org/10.1186/1756-3305-3-104> (2010).
38. Elmore, S. Apoptosis: a review of programmed cell death. *Toxicol. Pathol.* **35**, 495–516. <https://doi.org/10.1186/1756-3305-3-104> (2007).
39. Farquhar, M. G. & Palade, G. E. The Golgi apparatus: 100 years of progress and controversy. *Trends Cell Biol.* **8**, 2–10. [https://doi.org/10.1016/s0962-8924\(97\)01187-2](https://doi.org/10.1016/s0962-8924(97)01187-2) (1998).
40. Machamer, C. E. Golgi disassembly in apoptosis: cause or effect?. *Trends Cell Biol.* **13**, 279–281. [https://doi.org/10.1016/s0962-8924\(03\)00101-6](https://doi.org/10.1016/s0962-8924(03)00101-6) (2003).
41. Macedo-Silva, S. T., Urbina, J. A., Souza, W. J. & Rodrigues, J. C. F. In vitro activity of the antifungal azoles itraconazole and posaconazole against *Leishmania amazonensis*. *PLOS ONE* **8**, 1–14. <https://doi.org/10.1371/journal.pone.0083247> (2013).
42. Ogbadoyi, E. O., Robinson, D. R. & Gull, K. A high-order trans-membrane structural linkage is responsible for mitochondrial genome positioning and segregation by flagellar basal bodies in trypanosomes. *Mol. Biol. Cell* **14**, 1769–1779. <https://doi.org/10.1091/mbc.E02-08-0525> (2003).
43. Brandão, L. N. B. *et al.* Anti-malarial activity and toxicity of *Aspidosperma nitidum* Benth: a plant used in traditional medicine in the Brazilian Amazon. *Res. Soc. Dev.* **9**, 2–23. <https://doi.org/10.33448/rsd-v9i10.8817> (2020).
44. Vale, V. V. *et al.* Anti-malarial activity and toxicity assessment of *Himatanthus articulatus*, a plant used to treat malaria in the Brazilian Amazon. *Malar. J.* **14**, 1–10. <https://doi.org/10.1186/s12936-015-0643-1> (2015).
45. Mota, E. F. *et al.* Biological activities of *Croton palanostigma* Klotzsch. *Pharmacogn. Mag.* **11**, 1–6. <https://doi.org/10.4103/0973-1296.176109> (2015).
46. Silva, R. R. P. *et al.* In vitro biological action of aqueous extract from roots of *Physalis angulata* against *Leishmania (Leishmania) amazonensis*. *Complement. Altern. Med.* **15**, 2–10. <https://doi.org/10.4103/0973-1296.176109> (2015).

Acknowledgements

The authors are grateful to the Brazilian agencies Conselho Nacional de Desenvolvimento Científico e Tecnológico (CNPq), Comissão de Aperfeiçoamento de Pessoal de Nível Superior (CAPES), and Fundação Amazônia de Amparo a Estudos e Pesquisas (FAPESPA) for providing financial support for this study. Authors also would like to thank the laboratory technician Fernanda Brasil dos Santos Lobo for the technical support given for the development of the electron microscopy tests.

Author contributions

M.F.D. and F.T.S. were responsible for conception and design of the work. A.S.S.V. was responsible for in vitro experiments and phytochemistry study. A.S.S.V., S.C.A., E.O.S. and J.A.P.D.J. were responsible for morphological analysis. A.M.R.M., G.C.B. and V.V.V. were responsible for phytochemistry study. A.S.S.V., F.T.S., E.O.S. and M.F.D. were responsible for analysis and interpretation of results, writing and reviewing the manuscript. M.F.D., S.P. and M.B.C. were responsible for critical revision of the manuscript. All authors read and approved the manuscript.

Competing interests

The authors declare no competing interests.

Additional information

Correspondence and requests for materials should be addressed to M.F.D.

Reprints and permissions information is available at www.nature.com/reprints.

Publisher's note Springer Nature remains neutral with regard to jurisdictional claims in published maps and institutional affiliations.



Open Access This article is licensed under a Creative Commons Attribution 4.0 International License, which permits use, sharing, adaptation, distribution and reproduction in any medium or format, as long as you give appropriate credit to the original author(s) and the source, provide a link to the Creative Commons licence, and indicate if changes were made. The images or other third party material in this article are included in the article's Creative Commons licence, unless indicated otherwise in a credit line to the material. If material is not included in the article's Creative Commons licence and your intended use is not permitted by statutory regulation or exceeds the permitted use, you will need to obtain permission directly from the copyright holder. To view a copy of this licence, visit <http://creativecommons.org/licenses/by/4.0/>.

© The Author(s) 2022